Spatially modulated ephrinA1:EphA2 signaling increases local contractility and global focal adhesion dynamics to promote cell motility

Zhongwen Chen[a,b,1], Dongmyung Oh[b,1], Kabir H. Biswas[b,c], Cheng-Han Yu[d], Ronen Zaidel-Bar[b,e,2], and Jay T. Groves[a,b,2]

[a]Department of Chemistry, University of California, Berkeley, CA 94720; [b]Mechanobiology Institute, National University of Singapore, 117411 Singapore, Singapore; [c]School of Materials Science and Engineering, Nanyang Technological University, 639798 Singapore, Singapore; [d]School of Biomedical Sciences, Li Ka Shing Faculty of Medicine, The University of Hong Kong, Hong Kong, China; and [e]Department of Cell and Developmental Biology, Sackler Faculty of Medicine, Tel Aviv University, 69978 Tel Aviv, Israel

Edited by Jennifer Lippincott-Schwartz, Howard Hughes Medical Institute–Janelia Research Campus, Ashburn, VA, and approved May 4, 2018 (received for review November 16, 2017)

Recent studies have revealed pronounced effects of the spatial distribution of EphA2 receptors on cellular response to receptor activation. However, little is known about molecular mechanisms underlying this spatial sensitivity, in part due to lack of experimental systems. Here, we introduce a hybrid live-cell patterned supported lipid bilayer experimental platform in which the sites of EphA2 activation and integrin adhesion are spatially controlled. Using a series of live-cell imaging and single-molecule tracking experiments, we map the transmission of signals from ephrinA1:EphA2 complexes. Results show that ligand-dependent EphA2 activation induces localized myosin-dependent contractions while simultaneously increasing focal adhesion dynamics throughout the cell. Mechanistically, Src kinase is activated at sites of ephrinA1:EphA2 clustering and subsequently diffuses on the membrane to focal adhesions, where it up-regulates FAK and paxillin tyrosine phosphorylation. EphrinA1:EphA2 signaling triggers multiple cellular responses with differing spatial dependencies to enable a directed migratory response to spatially resolved contact with ephrinA1 ligands.

lipid bilayer | single molecule | Src | microfabrication | metastasis

Eph receptors and ephrin ligands form juxtacrine signaling complexes in the intercellular interface. Among all 16 Eph receptors, EphA2 is notorious for its high expression levels in most aggressive breast cancers (1, 2). There is, however, a long-standing debate concerning the role of EphA2 in cancer progression. Many published results may at first seem contradictory. For instance, overexpression of nonmutated EphA2 is sufficient to induce tumorigenesis and metastasis in nontransformed mammary epithelial cells (3), and has been shown to be associated with poor patient prognosis (4–6). Consistent with this, EphA2-deficient cells from knockout mice exhibit significantly reduced invasion and migration potential (7). On the other hand, activation of EphA2 by ephrinA1 ligand has been shown to attenuate Ras activation (8), suppress the Akt–mTORC1 pathway (9), and inhibit cell migration (10–12). As a possible resolution to this apparent contradiction, recent studies have suggested a ligand-independent mechanism that activates EphA2 promigratory signaling (13–16). Modulating the balance between ligand-dependent and ligand-independent pathways can significantly alter the overall cellular response. While this is a promising insight toward unraveling the paradoxical roles of EphA2 in cancer, a clear understanding of the role of ligand-dependent EphA2 signaling remains unresolved.

In addition to biochemical elements of EphA2 signaling, recent work using patterned supported lipid bilayers (SLBs) has revealed that the cellular response to EphA2 activation is modulated by the spatial distribution of its ephrinA1 ligand (17–19). EphA2 and ephrinA1 natively interact across the junctions between apposed cells. This juxtacrine signaling interface can be reconstituted between EphA2-expressing live cells and SLBs functionalized with ephrinA1, which diffuses freely on the membrane surface. The fluid display of ephrinA1 is important because it enables assembly of ephrinA1:EphA2 complexes into signaling clusters, as would naturally occur between two living cells. When physical barriers, fabricated onto the underlying substrate (20, 21), are applied to restrict the movement and assembly of ephrinA1:EphA2 complexes on SLBs, changes to the cellular response to EphA2 signaling are observed, including altered cytoskeleton morphology, blocked recruitment of the protease ADAM10, and hindered transendocytosis of ephrinA1 (17–19). We hypothesize that some of the apparent contradiction in the literature reports on the biology of EphA2 signaling may result from unseen spatial and mechanical aspects of signal modulation in this system.

In the present work, we focus on the effect of EphA2 signaling on integrin-mediated adhesions in a spatially defined manner. Cell migration is a coordinated process involving both the formation and dissociation of focal adhesions (FAs), sites of integrin-mediated cell attachment with the extracellular matrix (22). EphA2 receptor signaling has long been known to exhibit modulatory control over integrin functions. However, the nature of this regulation remains unclear. For example, a group of studies have reported that ephrin activation of EphA2 and other Eph receptors

Significance

Cell receptors are neither uniformly distributed nor uniformly activated across plasma membrane. However, very little is known about how their spatial arrangement affects cellular response to receptor signaling. EphA2 is a receptor tyrosine kinase whose activation depends on binding of EphrinA1 ligands on the opposing cell, and EphA2 signaling plays an important role in cancer metastasis. In adherent cells, integrin adhesions are a key element to regulate cell–matrix interactions and cell migration. However, our understanding of how their activities are spatiotemporally coordinated remains superficial. In this study, we combined microfabrication, live imaging, and single-molecule tracking to directly map the signal transduction from ephrinA1:EphA2 complex to integrin adhesions, and revealed a spatially controlled mechanism for EphA2–integrin signaling cross talk.

Z.C., R.Z.-B., and J.T.G. designed research; Z.C., D.O., and K.H.B. performed research; C.-H.Y. contributed new reagents/analytic tools; Z.C., D.O., R.Z.-B., and J.T.G. analyzed data; and Z.C., R.Z.-B., and J.T.G. wrote the paper.

The authors declare no conflict of interest.

This article is a PNAS Direct Submission.

[1]Z.C. and D.O. contributed equally to this work.

[2]To whom correspondence may be addressed. Email: jtgroves@lbl.gov or zaidelbar@tauex.tau.ac.il.

This article contains supporting information online at www.pnas.org/lookup/suppl/doi:10.1073/pnas.1719961115/-/DCSupplemental.

Published online June 4, 2018.

leads to dephosphorylation of focal adhesion kinase (FAK) and exerts a negative influence on integrin-mediated adhesions (10–12, 23–25). In other studies, activated EphA2 and other Eph receptors have been reported to enhance phosphorylation of FAK and promote cell spreading (26–29). Although there are many possible reasons for these seemingly contradictory results, a widely neglected factor is the spatial control of ephrinA1:EphA2 interactions. While most studies have used soluble or surface-coated ephrinA1 ligands to trigger the cell in a global way, the naturally formed ephrinA1:EphA2 interactions at physiological cell–cell junctions are spatially separated from cell–matrix adhesions (30). Thus, we speculate that spatial arrangement may be an important factor influencing EphA2–integrin signaling cross talk.

In this study, we developed a micropatterned hybrid substrate with ephrinA1 ligands presented on fluid SLB corrals embedded within regions of immobilized Arg–Gly–Asp (RGD) peptides. The regions of immobilized RGD function both as integrin ligands (31) and lipid bilayer diffusion barriers (20, 21, 32, 33). This configuration permits fluid rearrangement, clustering, and activation of EphA2 receptors on the membrane regions. Simultaneously, mechanically mediated FA formation occurs on rigid regions of the substrate, enabling cell spreading. The sites of ephrinA1:EphA2 interactions and integrin adhesions are thus spatially separated to better mimic in vivo organization.

With this spatially resolved experimental setup, we find that activation of EphA2 by ephrinA1 promotes cell motility by inducing local contractions and increasing global FA dynamics. These results were obtained through an extensive series of live-cell imaging and single-molecule tracking experiments in which we directly image the spatial localization, dynamics, and transport of signaling molecules in response to ephrinA1 activation of EphA2 in live cells. Specifically, we observed Src kinase activation at sites of EphA2 triggering. After release from EphA2 clusters, Src diffuses on the membrane and becomes localized to FAs, where it up-regulates FAK and paxillin tyrosine phosphorylation. We suggest that this diffusive transport of Src through the membrane is the mechanism by which EphA2 modulates FA dynamics over long distances. Locally, ephrinA1:EphA2 triggering activates myosin-mediated contraction. Overall, we found that the EphA2 signaling system triggers multiple cellular processes with differing spatial dependencies—some more localized than others. The net effect is that the overall cellular behavior is sensitive to the spatial location of ephrinA1 ligands. Polarized activation of EphA2 receptors results in a migratory phenotype.

Results

Development of a Hybrid Substrate of Fluid EphrinA1 and Immobilized RGD. To investigate the signaling cross talk between EphA2 and integrin in a spatially resolved manner, we reconstituted EphA2 and integrin interactions with membrane-bound ephrinA1 and substrate-bound RGD. This is accomplished by developing a hybrid substrate containing SLB corrals micropatterned on a glass surface that is otherwise coated with biotinylated poly-L-(lysine)-grafted-polyethylene(glycol) polymer (PLL-PEG-biotin), at 1-μm spatial resolution (Fig. 1*A*). Alexa 680-labeled ephrinA1 was linked to the SLB through Ni^{2+}-NTA chelation (34). The density of ephrinA1 on the SLB is controllable over a range of $1–10^3$ molecules per square micrometer. Delight405-labeled NeutrAvidin and biotinylated RGD were linked to the PLL-PEG-biotin–coated area successively. Fluorescence recovery after photobleaching experiments confirmed that ephrinA1 was fluid on the SLBs (*SI Appendix*, Fig. S1 *A* and *B*). As a first test here, circular-shaped SLB corrals with 2-μm diameter were embedded within regions of immobilized RGD, with almost no cross binding (Fig. 1*B*).

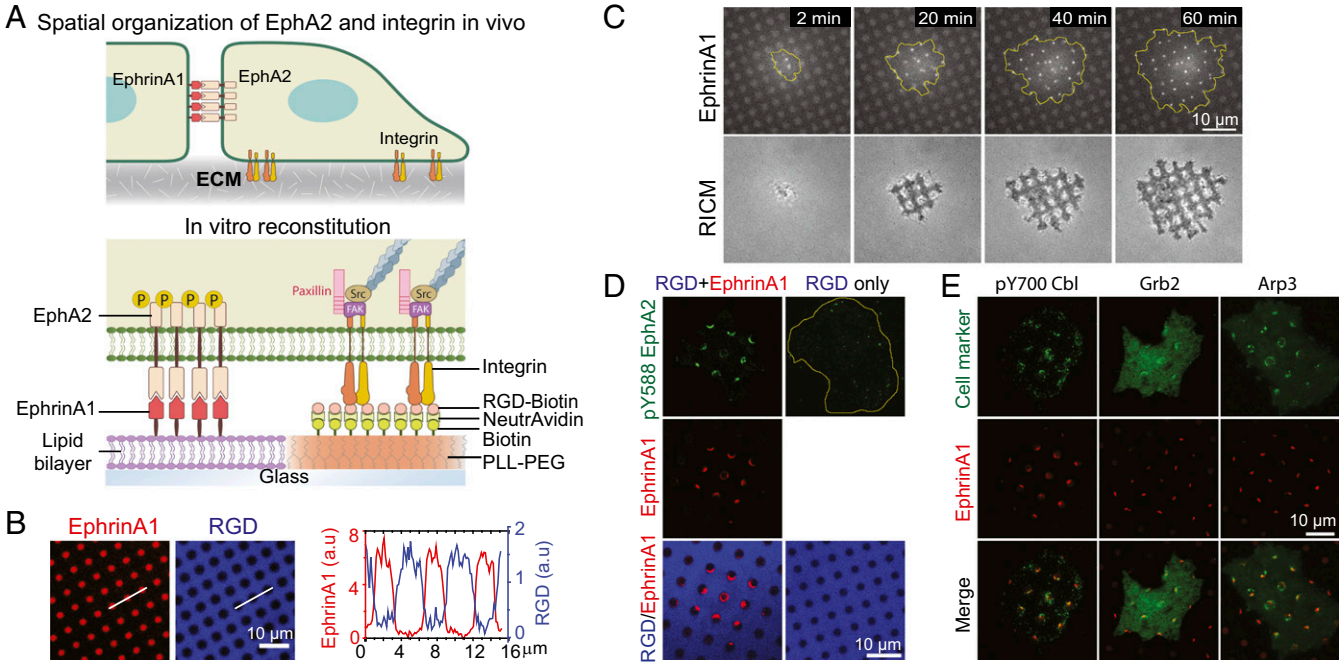

Fig. 1. Spatially controlled activation of EphA2 and integrin on a micropatterned hybrid substrate of fluid ephrinA1 and immobilized RGD. (*A*) Schematic illustration of the in vivo spatial organization of EphA2 and integrin and the in vitro reconstitution system. (*B*) Hybrid substrate images (*Left*) and intensity line profile (*Right*). (*C*) Time-course images of a cell spreading on the hybrid substrate. Yellow lines mark cell outlines, and RICM stands for "reflection interference contrast microscopy" images. (*D*) Fluorescent images of pY588-EphA2 of cells fixed after spreading for 30 min. RGD-only refers to the hybrid substrate of RGD and SLB, and RGD+EphrinA1 refers to the same substrate but with ephrinA1 on SLB. Pearson's correlation coefficient between pY588 EphA2 and ephrinA1 is 0.91 ± 0.05 (mean ± SEM). $n = 5$ cells. (*E*) Fluorescent images of different cellular proteins colocalized with ephrinA1 clusters. pY700-Cbl image is of a fixed cell that was immunostained after 60 min of spreading. Grb2-tdEOS and Arp3-mcherry are live-cell images after 60 min of spreading. Pearson's correlation coefficients between pY700-Cbl, Grb2, and Arp3, and ephrinA1 signals are 0.52 ± 0.04, 0.87 ± 0.06, and 0.55 ± 0.05 (mean ± SEM) respectively. $n = 5$ cells.

Formation of EphrinA1:EphA2 Signaling Clusters in Spreading Cells. The MDA-MB-231 breast cancer cell line was used in this study since it expresses a high level of the EphA2 receptor and is highly metastatic (1, 18). However, corroborative studies were also performed in an invasive prostate cancer cell line PC3 and a non-metastatic human breast epithelial cell line MCF10A. Cells were serum starved overnight to reduce other receptor signaling, detached from the culture plate with a nonenzymatic dissociation buffer, and then seeded on the hybrid substrates for further experiments.

As a first test, a minimal amount of ephrinA1 ligands, at a density of <5 molecules per square micrometer, was functionalized on the SLB corrals. The integrin ligand RGD facilitated isotropic cell spreading. Whenever the cell membrane touched a new SLB corral, almost all of the ephrinA1 molecules within this corral were rapidly concentrated into a single cluster (Fig. 1*C* and Movie S1). As a negative control, membrane-bound GFP did not induce any clustering (*SI Appendix*, Fig. S1*C*), confirming this specific to ephrinA1 ligands. Cells failed to spread when RGD was not presented on the polymer, although ephrinA1 was still clustered (*SI Appendix*, Fig. S1*D*).

In subsequent experiments, ephrinA1 density was increased to a physiological level of about 150–200 molecules per square micrometer on SLBs (17). The clustering of ephrinA1 ligands was paralleled by clustering and activation of EphA2 receptors within the cell, as shown by colocalization of anti-EphA2 and anti-phosphotyrosine antibodies in immunofluorescence images (*SI Appendix*, Fig. S1 *E* and *F*). On RGD-only control where ephrinA1 is not present on SLBs, no enrichment of EphA2 receptors was observed and phosphotyrosine only located in FAs and focal complexes at the periphery of the cell. EphA2 is known to undergo phosphorylation at tyrosine 588 upon ligand binding (35). Using a previously validated pY588-EphA2–specific antibody, we found a robust activation of EphA2 receptors in cells following 1 h of contact with RGD+EphrinA1 substrate both by immunofluorescence (Fig. 1*D*) and Western blot (*SI Appendix*, Fig. S1*G*). We further validated the activation of EphA2 signaling by observing the recruitment of known downstream effectors to the ephrinA1:EphA2 clusters, including the endocytosis marker phosphor-Cbl (36), the signaling adaptor Grb2 (37), and the actin nucleator Arp3 (38) (Fig. 1*E*). All of these results confirmed that the presentation of ephrinA1 on fluid SLB is a potent method to activate highly specific EphA2 signaling. The dynamical aspects of ephrinA1 interaction with EphA2, as well as the timescale of downstream events, can be mapped quantitatively with this system.

EphrinA1 Changes Cell-Spreading Behavior by Inducing Retractions and Protrusions. The hybrid substrate spatially separates ephrinA1:EphA2 interactions and integrin-mediated cell adhesions, and thus can be used to parse out spatial effects of EphA2 signaling on cell spreading and movement. Cell spreading on a flat and uniform adhesive surface is usually isotropic at first, followed by cellular polarization over the next several hours (39,

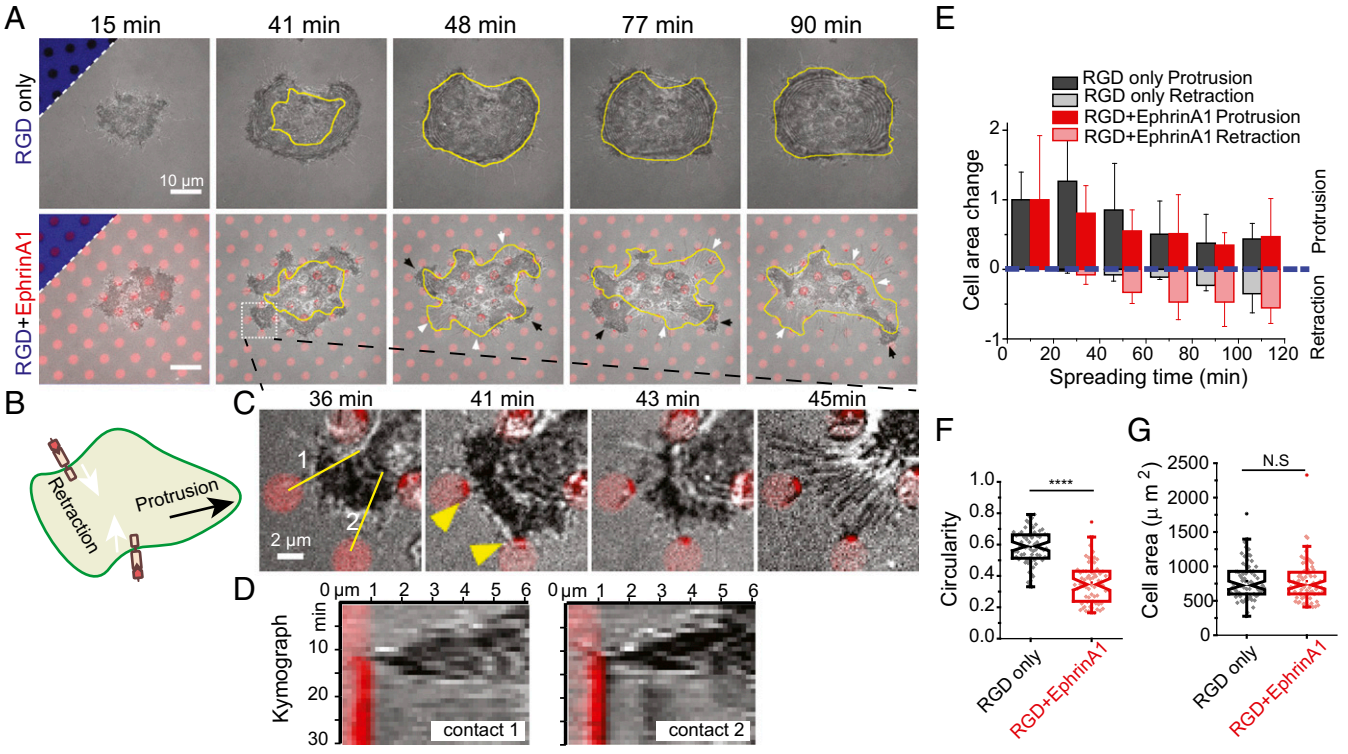

Fig. 2. EphA2 activation changes cell-spreading behavior by inducing retractions and protrusions. (*A*) Time-course images of cells spreading either on RGD-only or RGD+EphrinA1 substrates. The substrate has a circular shape of SLB with diameter of 3 μm and center-to-center distance of 9 μm. All images are superposition of the RICM and ephrinA1 channels. The triangular *Insets* in the *Upper Left* corners of the first time point represent the underlying substrates. The closed yellow lines represent the outline of the cell in the previous time frame. White arrows indicate regions of retractions, and black arrows indicate regions of protrusions. (*B*) Illustration of ephrinA1:EphA2 interaction triggering local cell retraction and distant protrusion. (*C*) Zoom-in images of *A* highlighting local retractions. Yellow arrowheads indicate formation of ephrinA1 clusters. (*D*) Kymographs constructed from lines 1 and 2 in *C*. (*E*) Quantification of cell area change, with positive value representing protrusion and negative value representing retraction. Cell area change was measured by the protruded or retracted area compared with the cell 20 min ago, as illustrated in *SI Appendix*, Fig. S2*A*. The change of cell area is normalized by the total cell area at its first time point for individual cells. For the first time point ($t = 10$ min), data are shown as the total cell area itself. Data are presented as average bar ± SD. $n = 6$ for RGD+EphrinA1 and $n = 5$ for RGD-only groups. (*F* and *G*) Quantification of (*F*) cell circularity and (*G*) cell area after 90 min of spreading on indicated substrates. Data are presented as Notch box plus individual points overlay; $n = 70$. ****$P < 0.0001$ for Student's t test.

40). Similarly, serum-starved MDA-MB-231 cells, plated on a substrate with RGD surrounding pure SLB corrals, spread uniformly for about 40 min, after which their edges remained relatively quiescent. In contrast, cells spreading on the hybrid substrate with ephrinA1 on the SLB displayed very anisotropic dynamics; while some regions of the cell underwent prominent protrusions, other regions exhibited dramatic retractions (Fig. 2 *A* and *B* and Movie S2). Closer examination of the live-cell movies revealed that each retraction correlated with a local ephrinA1 clustering event. As shown in the example in Fig. 2 *C* and *D*, immediately after a lamellipodial protrusion touched a SLB corral, ephrinA1 formed a cluster at the contact point, and a few minutes thereafter the cell protrusion strongly retracted toward the cell body, often leaving behind retraction fibers that remained connected to the ephrinA1 cluster.

Initial cell spreading can be further divided into two phases depending on myosin activities: noncontractile spreading followed by contractile spreading (40). As observed here, in the first 40 min, cells rapidly increased their contact area without generating retractions both in RGD-only and RGD+EphrinA1 substrates, corresponding to noncontractile spreading phase (Fig. 2*E* and *SI Appendix*, Fig. S2*A*). Dynamic retractions and protrusions only began after cells passed the rapid spreading phase in the presence of ephrinA1, suggesting that ephrinA1-induced retractions involve myosin activities, which will be discussed in the next section. This dynamic behavior persisted for as long as we imaged the cells (~3 h) and resulted in changes in cell shape, as measured by a significant reduction in cell circularity after 90 min of spreading (Fig. 2*F*). Interestingly, in contrast to previous studies, in which triggering EphA2 signaling with soluble or surface-coated Fc-ephrinA1 led to cell rounding and a reduction in cell spreading (10, 11), we found the cell-spread area to be the same on the hybrid substrate with or without ephrinA1 (Fig. 2*G*).

We repeated these experiments with PC3 and MCF10A cells. Both cells also showed continuous retractions and protrusions during spreading, although at different degrees, suggesting this to be a general cell behavior in response to such stimulations (*SI Appendix*, Fig. S2*B* and Movie S3).

EphrinA1 Induces Local Retraction Through Myosin II Activation. Nonmuscle myosin II was implicated in the cellular retractions by immunostaining cells with an antibody that recognizes the active form of myosin light chain (pSer19-MLC). Active MLC was largely located around the cell periphery both on control substrates and in the presence of ephrinA1, but it was significantly enhanced in regions that came into contact with ephrinA1 (Fig. 3 *A* and *B*). MLC-GFP live-cell imaging showed that cells experienced multiple events of a local increase in MLC fluorescence intensity followed by a local retraction during the overall spreading process on RGD+EphrinA1 substrate (*SI Appendix*, Fig. S3*A* and Movie S4). A typical retraction involved two phases: In the first phase, MLC accumulated locally after contact with ephrinA1, but the cell edge remained in place. After a certain threshold, the cell underwent a quick retraction phase, possibly because of a sudden loss of cell–matrix adhesions (*SI Appendix*, Fig. S3*B*). To clearly establish the temporal relationship between EphA2 activation and MLC accumulation, we seeded cells on a substrate with a large area of RGD embedded with small ephrinA1 SLB corrals (Fig. 3*C*). Movie S5 shows the events that occurred when a cell spread on the RGD region first touched one patch of ephrinA1. EphrinA1 clustering by a filopodial contact clearly preceded MLC local accumulation (Fig. 3*C* and *SI Appendix*, Fig. S3*C*), suggesting MLC is a downstream effector of EphA2 signaling.

The involvement of nonmuscle myosin II in ephrinA1-induced cell retraction was further confirmed by pharmacological inhibition. After treatment with 10 μM of the myosin II inhibitor blebbistatin, at a time point when the cell was transiently retracting, it stopped retracting and spread out isotropically without forming any new retractions, even after contact with new ephrinA1 SLB corrals (Fig. 3 *D* and *E*). Taken together, we conclude that myosin II is locally activated following stimulation by ephrinA1.

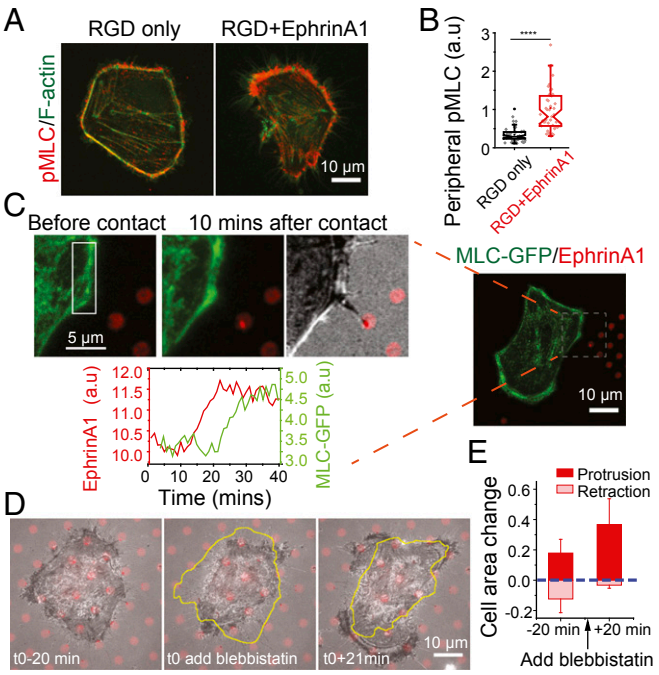

Fig. 3. EphA2-induced local retractions is dependent on myosin II activation. (*A* and *B*) EphrinA1 stimulation increases peripheral myosin light chain (MLC) phosphorylation. (*A*) Immunofluorescence images of pSer19-MLC and F-actin of cells fixed after 90 min of spreading on indicated substrates. (*B*) Quantification of peripheral pMLC intensities. Data are presented as Notch box plus individual points overlay. $n = 48$ for RGD-only sample; $n = 45$ for RGD+EphrinA1 sample. ****$P < 0.0001$ for Student's t test. (*C*) A MLC-GFP–transfected cell spread on a large RGD area where only one patch of ephrinA1 is engaged by a filopodial contact. Time-course fluorescence intensity graph shows the local MLC-GFP changes [selected region of interest (ROI)] by a single ephrinA1 cluster stimulation. (*D*) Cell spreading on the hybrid substrate before and after blebbistatin treatment. The closed yellow lines represent the outline of the cell in the previous time frame. (*E*) Quantification of cell area change before and after blebbistatin treatment. The change of cell area is normalized by the total cell area 20 min before drug treatment for individual cells. Data are presented as average bar ± SD. $n = 6$.

EphA2 Activation Increases Focal Adhesion Dynamics Throughout the Cell. In addition to the myosin-dependent retractions, EphA2 signaling enhanced protrusive activities, which we reasoned might be the result of altered integrin adhesion dynamics. Previous studies addressing the impact of EphA2 signaling on integrin function have yielded contradictory results (as discussed in the Introduction). The system we developed here is more physiological in the sense that EphA2 and integrin ligands are spatially separated, and ephrinA1 is presented on a fluid membrane (Fig. 4*A*). Taking advantage of this setup, we map the functional effects of EphA2 signaling on integrin-mediated FAs.

First, we immunostained cells with a paxillin antibody to observe FA morphology. In cells spreading on RGD-only substrate for 90 min, FAs were found both in the periphery of the cell as well as some distance toward the center, connected with long and clear actin stress fibers (Fig. 4*B*). In contrast, FAs were closer to the cell edge in the presence of ephrinA1 (Fig. 4*C*), and the stress fibers were less continuous. The total number of FAs per cell decreased in the presence of ephrinA1 (Fig. 4*D*), but not FA size (*SI Appendix*, Fig. S4*A*) or FA aspect ratio (*SI Appendix*, Fig. S4*B*). It is important to note that a minimal size thresholding was used in

image analysis to extract FAs from image background, and thus small nascent adhesions were excluded in this quantification.

To understand the origin of the differences we observed in static images, cells were transfected with paxillin-GFP to visualize FAs by total internal reflection fluorescence (TIRF) microscopy. Because of high signal-to-noise ratio in TIRF live-cell imaging, all paxillin-GFP recruitment events were counted for analysis, including small nascent adhesions. Movies were recorded starting 50 min after seeding, by which time most cells developed mature FAs. Results revealed a striking difference in paxillin-GFP dynamics, wherein adhesions all over the cell were significantly more dynamic in the presence of ephrinA1 compared with the RGD-only control (Movie S6). As shown in lifetime color-coded FA trajectories, all FAs have a much shorter lifetime on the substrate with ephrinA1 compared with control (Fig. 4*E* and *SI Appendix*, Fig. S4*C*). The distribution of every FA lifetime was then fitted with a second-order exponential decay function to get the characteristic lifetime per cell (Fig. 4*F*), which was compared among a group of cells (Fig. 4*G*). The average characteristic lifetime of FAs on RGD+EphrinA1 substrate (3.4 ± 0.7 min) is significantly shorter than the lifetime of FAs on RGD-only substrate (4.9 ± 1.2 min). However, a lot more small and fast turning-over adhesions formed on the RGD+EphrinA1 substrate (*SI Appendix*, Fig. S4*D*), resulting in a significantly higher FA formation rate (22.9 ± 9.9/min) compared with control (6.5 ± 2.2/min) (Fig. 4*H* and *SI Appendix*, Fig. S4 *E* and *F*). This suggests that EphA2 signaling not only leads to FA disassembly but also promotes their formation. Taken together, our results show that EphA2 signaling increases FA dynamics throughout the cell. On RGD-only substrate, new adhesions form in the periphery of cells and move centripetally

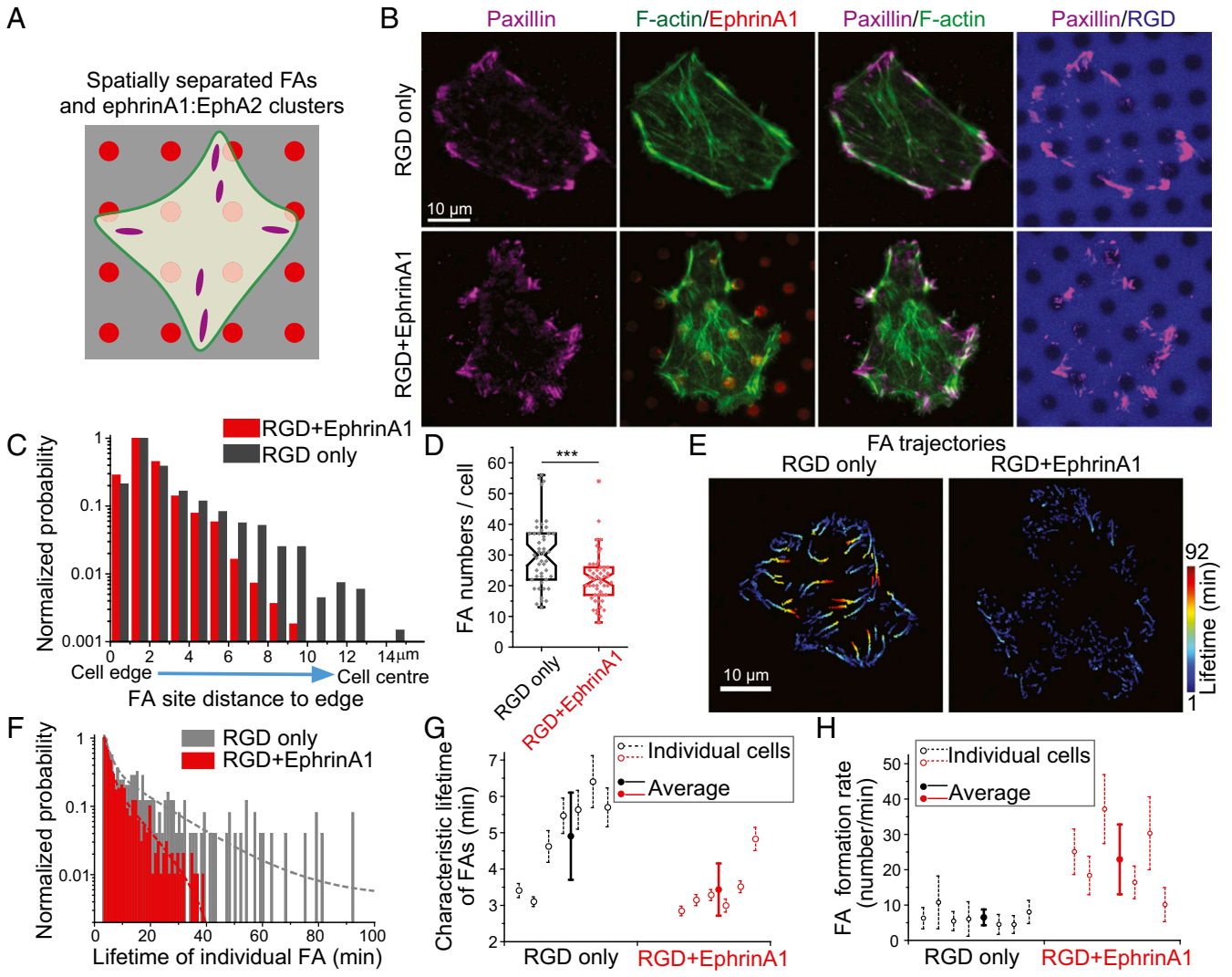

Fig. 4. EphA2 signaling increases FA dynamics. (*A*) FAs and ephrinA1:EphA2 clusters are spatially separated in the hybrid substrate. (*B*) Immunofluorescence images of paxillin and F-actin of cells fixed after 90 min of spreading. (*C* and *D*) Quantification of FA distribution from cell edge to center (normalized by the highest probability in each group) (*C*) and FA numbers per cell, counted from $n = 47$ cells in RGD-only sample, and $n = 49$ cells in RGD+EphrinA1 sample (*D*). ***$P < 0.001$ for Student's t test. (*E*) Lifetime color-coded trajectories of paxillin-GFP of cells spreading on indicated substrates. TIRF images were taken after 50 min of spreading, at a rate of 1 frame per minute for a total of 92 min. Lifetime color-coded paxillin adhesion centroids were plotted and assembled from all images to reflect FA trajectories. Adhesions are blue when they appear, and over time they gradually change toward red until disappearing. (*F–H*) Quantifications of FA lifetime and formation rate. (*F*) Distribution of the lifetime of all individual FAs in the two cells tracked in *E*. Lifetime distribution was fitted with second-order exponential decay function to get characteristic time constant τ2. (*G*) τ2 was compared in a group of cells. Data are presented as (τ2 ± fitting error) for individual cells, and (mean ± SD) for average values. (*H*) FA formation rate of cells on the two substrates. Data are presented as (mean ± SD) for both individual cells and average values.

over a long time, whereas in RGD+EphrinA1 substrate, those adhesions disassemble before they can move to the center, which explains the localization difference quantified from immunostaining images (Fig. 4*C*).

Outward integrin trafficking from cytosol to plasma membrane has been reported in immune cells after ligand stimulation to enhance cell–cell or cell–substrate adhesions (41–44), but integrin trafficking is not affected by EphA2 signaling in MDA-MB-231 cells as monitored by probes for β1 integrin (*SI Appendix*, Fig. S5).

Src Kinase Is Recruited and Activated in EphrinA1:EphA2 Clusters. Src kinase is implicated as a signaling molecule connecting EphA2 with integrin, because it is a known downstream target of Eph receptors (28, 45) and is also a known regulator of FA dynamics (46–48) (Fig. 5*A*). Immunostaining with an antibody specific for the active state of Src (pY419-Src) (46) showed that Src was colocalized both in ephrinA1:EphA2 clusters and paxillin (Fig. 5*B*). On the control substrate, however, pY419-Src was mostly colocalized with paxillin only. Quantification of pY419-Src/EphA2 ratio in a range of circular patterns with SLB diameters

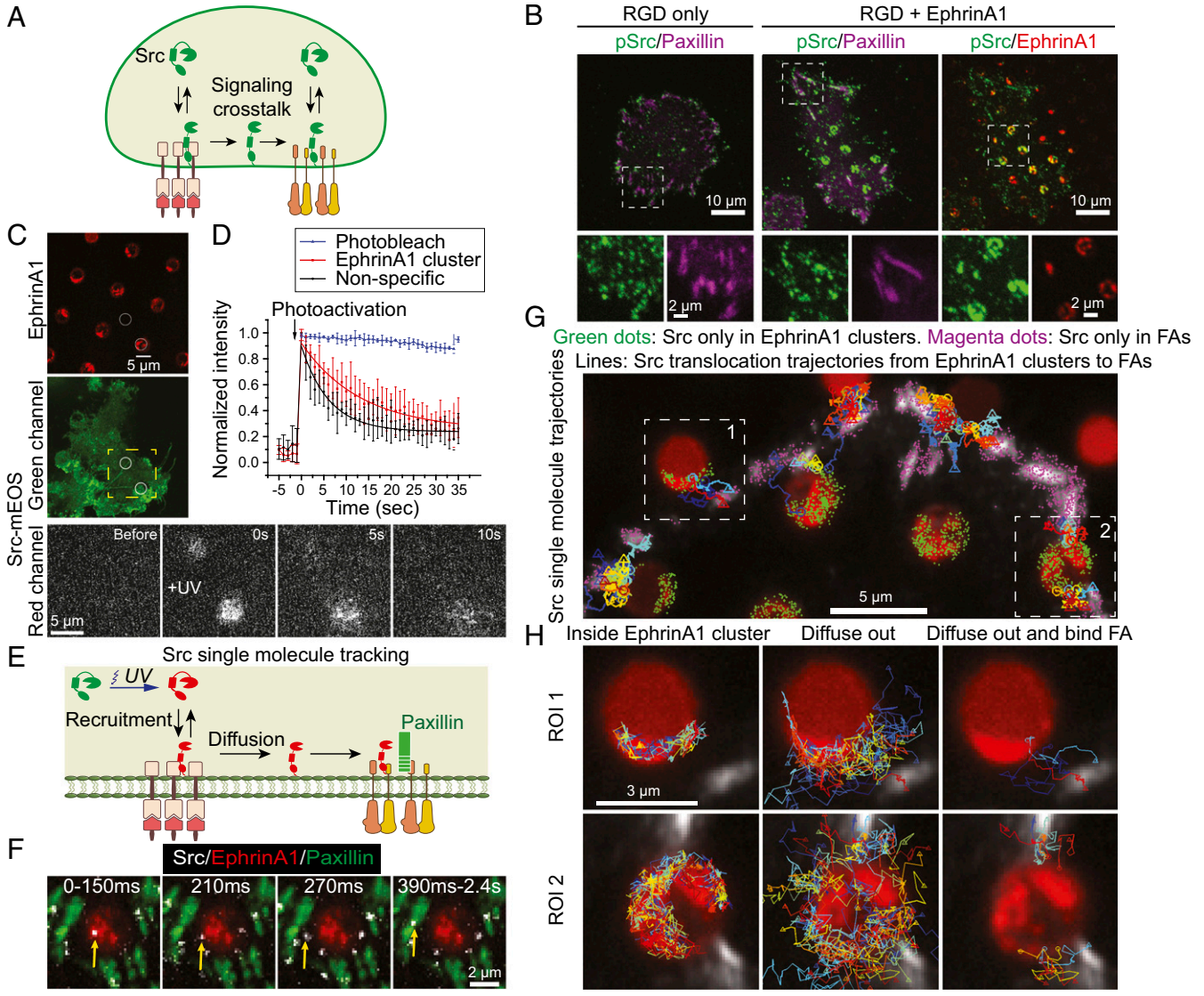

Fig. 5. Src kinase is recruited and activated in EphA2 clusters and then diffuses into FAs. (*A*) Src mediates signaling cross talk between EphA2 and integrin receptors. (*B*) Immunofluorescence images of pY419-Src and paxillin in cells fixed after 1 h of spreading on indicated substrates. (*C* and *D*) Photoactivation of Src-mEOS3.2 on cells spread on an RGD+EphrinA1 substrate. (*C*) A localized UV (405-nm) pulse was applied to simultaneously photoactivate Src-mEOS3.2 in one region of ephrinA1 clusters and one nonspecific region in the same cell (white circles). Src-mEOS3.2 red channel was recorded before and after UV exposure (selected ROI by a yellow square). (*D*) Graph of normalized Src-mEOS3.2 red fluorescence intensities in the circular regions. Photobleach control was acquired from bulk plasma membrane measurement with the same imaging acquisition settings. $n = 7$. (*E*) Principles of Src-mEOS3.2 single-molecule tracking in cells with cotransfection of paxillin-GFP and spread on Alexa 680-labeled ephrinA1 substrate. (*F*) One example of Src single-molecule tracking showing translocation from ephrinA1 clusters to FAs. The Src single-molecule movie and static images of FAs and ephrinA1 are merged to reveal Src recruitment and diffusion. Yellow arrow indicates a Src single molecule, with indicated recording time from its first appearance. (*G* and *H*) Src single-molecule trajectories. (*G*) Src molecules are recruited both in ephrinA1 clusters and FAs, which then dissociate in the same location or diffuse away through membrane. Green dots represent the initial location of Src single molecules that first appear in ephrinA1 clusters and then disappear in the same region. Magenta dots represent the initial location of Src single molecules that first appear in FAs and then disappear in the same region. Trajectory lines represent Src translocation from ephrinA1 clusters to FAs. (*H*) High-resolution Src single-molecule trajectories in two representative ROIs in *E*. Src molecules that first appear in ephrinA1 cluster region are divided into two groups: always inside ephrinA1 clusters or later diffusing outside. Among those diffusing outside molecules, a subpopulation bind FAs.

from 1 to 4 μm showed that pY419-Src molecule number is linearly correlated with EphA2 receptors across two orders of magnitude, confirming activation of Src by ephrinA1:EphA2 clustering (*SI Appendix*, Fig. S6 *A* and *B*). Importantly, pY419-Src intensity increased by about 15% in cell area excluding SLB regions in RGD+EphrinA1 group compared with RGD-only control (*SI Appendix*, Fig. S6*C*). Recruitment of Src-GFP to ephrinA1:EphA2 clusters was also visualized in live-cell imaging. An example from such a movie shows enrichment of Src-GFP when the cell made contact with an ephrinA1 SLB corral, but not in the case of Marina Blue-labeled SLB (*SI Appendix*, Fig. S6*D*).

Src Translocates from EphrinA1:EphA2 Clusters to FAs by Membrane Diffusion. Src is only activated on plasma membrane and its activity is known to increase FA turnover to promote cancer migration (47), so we hypothesize that Src links EphA2 activation to integrin adhesions by membrane diffusion. Experimentally, we took advantage of the hybrid substrate and single-molecule imaging to directly observe translocation of Src from ephrinA1:EphA2 clusters to FAs.

First, photoswitchable mEOS3.2-tagged full-length Src was used to reveal Src membrane diffusion. Src-mEOS3.2 red fluorescence was lighted up upon UV (405-nm) exposure in a region of ephrinA1 cluster and simultaneously in a nonspecific region, and then gradually diffused away (Fig. 5*C*). Src activation is dependent on binding of its SH2 domain to phosphorylated tyrosine residues on other proteins to release its closed autoinhibitory conformation (46). The slower decay rate of photoactivated Src from the ephrinA1 cluster region compared with the nonspecific region (Fig. 5*D*) suggests that Src dynamically binds EphA2 receptors and potentially becomes activated there, consistent with immunostaining results.

By controlling UV exposure time, we achieved single-molecule resolution to validate whether the same Src molecule recruited by EphA2 receptors can diffuse into FAs. In this experiment, cells were cotransfected with Src-mEOS3.2 and paxillin-GFP. mEOS3.2 and GFP have an overlap in green fluorescence spectrum; but because paxillin and Src colocalize in FAs, green fluorescence could still be used to highlight FA structures. Following a pulsed UV exposure, single-molecule movies of photoactivated Src-mEOS3.2 were recorded by TIRF microscopy (Fig. 5*E*). We confirmed Src-mEOS3.2 to be single molecules by observation of single-step photobleach and single-species distribution (*SI Appendix*, Fig. S7 *A* and *B*). Fig. 5*F* shows an example of a Src molecule that was recruited to the plasma membrane in an ephrinA1:EphA2 cluster region, dwelled there for 150 ms and then diffused into a nearby FA, and stayed there for nearly 2 s before dissociated or photobleached. More examples are shown in Movie S7. Importantly, the localized dwell events reflect specific interactions between Src-EphA2 and Src-FAs. This is a direct observation of recruitment, membrane diffusion, and translocation of single molecules from one receptor to another.

Detailed analysis of Src single-molecule trajectories showed that Src freely diffuses on the plasma membrane and can bind both EphA2 clusters and FAs. When a Src molecule initially appears in an ephrinA1:EphA2 cluster region or FAs region, it may dwell some time, and then dissociate in the same region or diffuse out (Fig. 5*G*). Importantly, a subset of Src molecules that diffused out of ephrinA1:EphA2 clusters subsequently reached FAs through Brownian motion and bound there. We detected multiple ephrinA1 clusters to FAs translocation events throughout the cell (Fig. 5 *G* and *H* and *SI Appendix*, Fig. S7*C*). Note that the detected trajectory length is limited by fluorophore photobleach time, which is typically less than a few seconds in this experimental condition. The diffusion coefficient of Src-mEOS on the plasma membrane was measured to be 0.41 ± 0.015 $\mu m^2/s$ (*SI Appendix*, Fig. S7 *D* and *E*), suggesting that Src molecules can diffuse throughout the cell in the timescale of a few minutes.

EphA2-Induced Increase in FA Dynamics Is Dependent on Src and FAK, and Correlates with Paxillin Phosphorylation. Next, the functional role of Src in EphA2-induced increase in FA dynamics was tested by drug inhibition and mutant expression (Fig. 6*A*). We applied 10 μM of the Src kinase inhibitor PP2 during cell spreading on the RGD+EphrinA1 hybrid substrate. Paxillin-GFP–transfected cells were imaged continuously before and after treatment with PP2. Before addition of the inhibitor, FA dynamics were very fast as shown earlier. However, after Src inhibition, adhesions were stabilized and resembled those of control cells (Fig. 6*B*, *SI Appendix*, Fig. S8*A*, and Movie S8). FA formation rate dropped immediately from 15.3 adhesions per minute predrug to 3.4 adhesions per minute after addition of PP2 (Fig. 6*C* and *SI Appendix*, Fig. S8*B*). In comparison, FA lifetime did not change after PP2 treatment in RGD control substrate, and FA formation rate only reduced slightly (*SI Appendix*, Fig. S8 *A* and *B*), suggesting that activated Src is responsible for both fast assembly and disassembly of FAs downstream of EphA2 activation.

These results were further validated by interfering with Src activity in a nonpharmacological manner. The standalone SH2 domain of Src competed with endogenous Src to bind FAs and EphA2 receptors (*SI Appendix*, Fig. S8*C* and Movie S9). Detailed analysis showed that tdEOS-tagged Src-SH2 was recruited to EphA2 immediately upon ephrinA1:EphA2 clustering (*SI Appendix*, Fig. S8*D*). However, since it lacks the Src kinase domain we reasoned that at high expression level it should act as a dominant-negative mutant and inhibit Src activity. Thus, we compared FA dynamics in cells expressing the Src-SH2-tdEOS on RGD+EphrinA1 or control substrates. In this experiment, FAs were marked directly by Src-SH2-tdEOS because they colocalize on RGD regions (*SI Appendix*, Fig. S8*E*). The characteristic lifetime (5.8 ± 1.9 min) and formation rate (5.3 ± 1.9/min) of FAs on the control substrate were similar to those measured using paxillin-GFP, indicating that Src-SH2-tdEOS expression did not perturb adhesion dynamics significantly under control conditions (Fig. 6 *D* and *E*). Remarkably, characteristic adhesion lifetime (5.2 ± 3.3 min) on the ephrinA1-containing substrates was almost the same as control (Fig. 6*D*), and formation rate (8.7 ± 7.7/min) only slightly increased in cells expressing Src-SH2-tdEOS (Fig. 6*E* and *SI Appendix*, Fig. S8*F*). Taken together, both drug treatment and Src-SH2 overexpression experiments prove that Src activation by EphA2 receptors is responsible for the increase of FA dynamics.

FAK is an important downstream target of Src that is known to regulate FA assembly and disassembly (49) (Fig. 6*F*). Western blot analysis revealed a significant increase in phosphorylation of tyrosine 576 of FAK, a Src-dependent phosphorylation site, on ephrinA1-containing substrate compared with control (Fig. 6*G*). Moreover, pharmacological inhibition of FAK using 10 μM PF573228 increased FA lifetime (Fig. 6*H* and *SI Appendix*, Fig. S9*A*) and decreased FA formation rate (Fig. 6*I* and *SI Appendix*, Fig. S9*B*) as measured in paxillin-GFP tracking on RGD+EphrinA1 substrate (Movie S10). The effect of FAK inhibition on FA stability (Fig. 6*H* and *SI Appendix*, Fig. S9*A*) is not as strong as Src inhibition, suggesting that FAK is not the only downstream target of Src to cause FA disassembly. Immunostaining images and live-cell imaging showed that FAK was only located in FAs (*SI Appendix*, Fig. S9 *C* and *D*), indicating that FAK is not directly phosphorylated by EphA2, but possibly downstream of Src. FAK-dependent tyrosine phosphorylation of paxillin is also known to enhance both FA assembly and turnover (50). Western blot result revealed a 50% increase in phosphorylation of tyrosine 118 of paxillin on the ephrinA1 substrate compared with control (Fig. 6*G*). Taken together, these results suggest an EphA2–Src–FAK–paxillin pathway to regulate FA dynamics.

Polarized Presentation of EphrinA1 Induces Directed Cell Migration. The isotropic distribution of ephrinA1 SLB corrals on our hybrid substrate was such that cells encountered ephrinA1 in

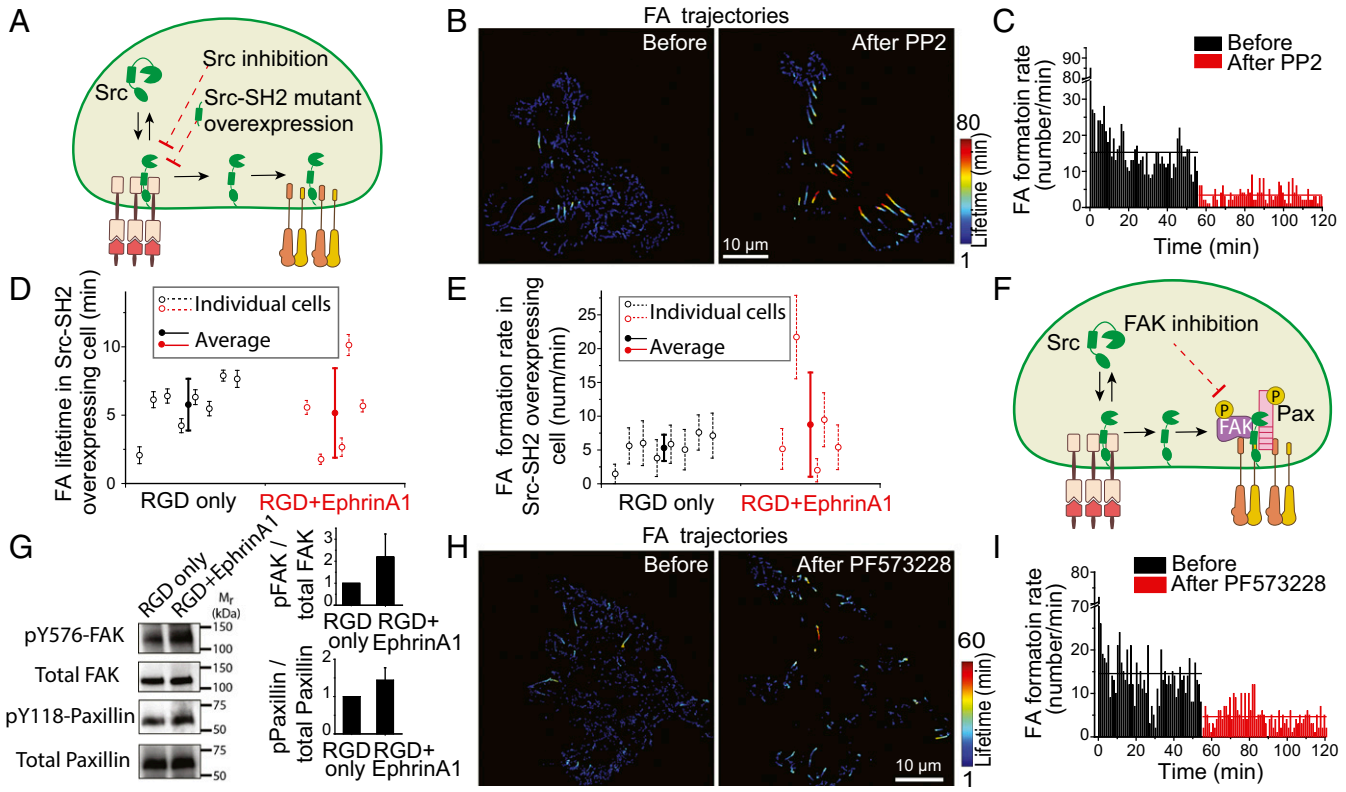

Fig. 6. EphA2-induced FA dynamics increase is dependent on Src and FAK, and is correlated with paxillin phosphorylation. (*A*) Perturbation of Src activity either by drug inhibition or overexpressing of dominant-negative mutant. (*B*) Lifetime color-coded trajectories of paxillin-GFP in a cell on RGD+ EphrinA1 substrate before and after Src inhibition. Ten micromolar PP2 was added into the media 55 min after the beginning of the recording. *Left* image shows paxillin-GFP trajectories from the first 55 min, and *Right* shows trajectories from 56 to 120 min. (*C*) Quantification of FA formation rate in the same cell shown in *B*, plotted with average values before and after PP2 treatment. (*D* and *E*) Quantifications of (*D*) FA lifetime and (*E*) formation rate in Src-SH2-tdEOS–overexpressing cells. (*F*) Src forms a complex with FAK and paxillin in FAs. FAK activity can be perturbed by drug inhibition. (*G*) Western blot of pY576-FAK, total FAK, pY118-paxillin, and total paxillin from cells lysed after 1 h of spreading on indicated substrates. Quantifications of pY576-total/total FAK and pY118-paxllin/total paxillin ratios were normalized with RGD-only control. $n = 3$. (*H*) Lifetime color-coded trajectories of paxillin-GFP in a cell on RGD+ EphrinA1 substrate before and after FAK inhibition. Ten micromolar PF573228 was added after 55 min of the movie. *Left* image is assembled from paxillin-GFP trajectories from the first 55 min. *Right* image is assembled from trajectories during 56–120 min. (*I*) Quantification of FA formation rate in the same cell shown in *F*, plotted with average values before and after PF573228 treatment.

every direction they protruded, and therefore despite their vigorous protrusions and contractions they did not effectively migrate in any direction. We reasoned that spatially restricted presentation of ephrinA1 will allow a polarized response to induce cell migration. As shown in Fig. 7*A* and Movie S11, we engineered a substrate on which cells adhering to RGD encounter ephrinA1 SLB corrals on only one side. Cells initially spread toward both sides isotropically on the RGD surface, but shortly after making contact with the SLB, they clustered ephrinA1 and retracted locally. Importantly, cell protrusion on the other side accelerated shortly after the formation of clusters (Fig. 7*B*), leading to a migration response triggered by this geometrical signal.

Discussion

Since the discovery of Eph receptors and their ligands almost 30 y ago (51, 52), their biological functions have been extensively studied, both in healthy development and diseases. However, the spatiomechanical aspects of regulation, which have recently emerged as important factors in many other ligand:receptor signaling systems (32, 53, 54), have been largely neglected in ephrin:Eph interaction studies. Ever since it was found that ephrin ligands require clustering for activity (55), Fc-IgG fused ephrin preclustered by antibodies has been used as a standard method to study Eph-related functions. However, the soluble ligands fail to recapitulate several aspects of the natural way by which Eph receptors interact with ephrin. First, soluble ligands are not presented on a membrane surface. This changes the mechanics of Eph receptor movement and clustering, which has previously been shown to modulate downstream activities including ADAM10 recruitment and receptor endocytosis (17, 19). Second, soluble ligands tend to activate cell surface receptors from every direction, which is not the case in a tissue context, where cell–cell and cell–matrix interactions are always spatially separated. For example, a proteomic study revealed systematic differences in protein phosphorylation levels in EphB2-expressing cells following stimulation either by soluble ephrinB1 ligand or by mixing ephrinB1-expressing cells (56), providing further evidence that the geometrical parameters are important in regulating Eph receptor functions. To better reconstitute EphA2 signaling, here we developed a hybrid substrate that preserves both the membrane context of ephrinA1 and spatial control. Our results showed that local activation of EphA2 receptors triggered a local increase in contractility, and a global increase in FA dynamics, a phenotype that is consistent with migratory behavior. As our results suggest, this cellular response is dependent on EphA2-mediated activation of Src, and possibly through the Src–FAK–paxillin signaling axis as shown in the proposed model (Fig. 7*C*).

EphA2-induced local retraction is possibly mediated through activation of a RhoGEF–RhoA pathway. It is evident that in neural development, a class of RhoGEF family named Ephexin

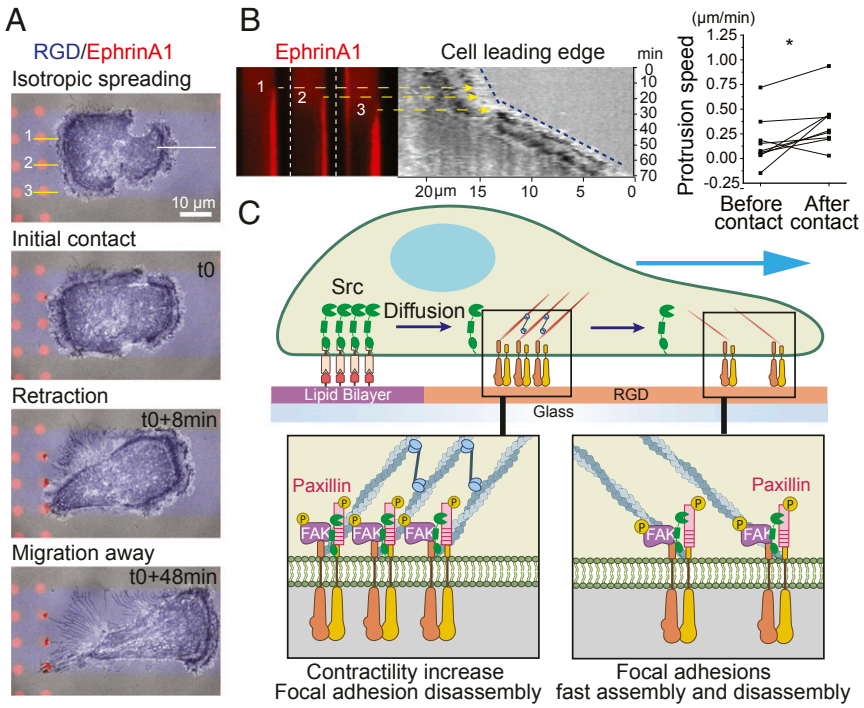

Fig. 7. Spatially controlled activation of EphA2 drives a local increase in contractility and a global increase in FA dynamics. (*A*) Time-course images of a cell spreading and migrating on a hybrid substrate. Cell is confined within a stripe of RGD (blue) separated by PEG (gray). EphrinA1 (red) presented SLB is only on one side of the stripe. (*B*, *Left*) Kymographs constructed from *A*. The three ephrinA1 clustering kymographs are constructed from yellow lines, and cell leading edge (blue dash line) is constructed from white lines in *A*. All kymographs are aligned in parallel with reference to time. The three yellow arrows point to the leading edge position at the time of each cluster initiation. (*Right*) Quantification of cell leading edge protrusion speed before and after ephrinA1 contact. $n = 9$. (*C*) Illustration of the proposed model.

is directly activated by Eph receptors to regulate growth cone collapse and synapse formation (57, 58). However, the expression level of Ephexin in cancers is very low. Which specific RhoGEF is downstream of EphA2 receptor in such a case is still an open question.

Our results demonstrate that EphA2 signaling not only increases FA disassembly but also promotes their formation. A significant increase of small, rapidly turning-over integrin adhesions was found in the hybrid substrate with ephrinA1. This increase in FA dynamics suggests that EphA2 signaling does not inhibit cell spreading, but rather it stimulates cell movement by continuously forming new adhesions and disassembling old ones. We also demonstrate that EphA2 signaling system is intrinsically sensitive to the spatial organization of activating ligand with polarized ligand presentation leading to directional cell migration. The differences between these observations and previous reports (10, 25, 28) may stem from the different experimental configurations. In the system described here, integrin:RGD interactions are spatially separated from ephrinA1:EphA2; they do not physically compete with each other. In contrast, ephrinA1 ligand displayed on solid surfaces intrinsically competes with integrin adhesions. Soluble ephrinA1 stimulation also differs dramatically, with EphA2 being uniformly ligated throughout the cell. We suggest that the clear spatial separation of integrin adhesions and ephrinA1:EphA2 clusters may more closely model the physiological situation in a tissue. In addition, compared with our previous experimental setup using only SLBs (19), introduction of integrin adhesion molecules effectively flattened cell membrane interface and enabled more confident identification of specific associations of cellular components with EphA2 clusters, including Src, Cbl, Grb2, and Arp3.

The EphA2 signaling-mediated increase in FA dynamics is dependent on Src. Inhibition of Src activity either by drug or overexpression of dominant-negative mutants did not alter FA dynamics significantly on RGD control substrate, but it dramatically reduced FA dynamics in the presence of ephrinA1. Our results suggest that Src forms an integrin/Src/FAK/paxillin complex in FAs, and Src-mediated phosphorylation of FAK and paxillin regulates adhesion turnover, consistent with previous studies (48, 59, 60). Importantly, we find that EphA2 receptors recruit and activate Src from the cytosol, which then diffuses away through the plasma membrane. The same Src molecule that comes from EphA2 clusters freely diffuses on the membrane and can directly bind FAs, linking EphA2 signaling and integrin signaling remotely. Potentially, the increased population of active Src generated by EphA2 receptor activation shifts FA assembly and disassembly balance to a more dynamic side. The monitoring of Src single-molecule translocation was enabled by the spatially resolved signaling interactions on the hybrid substrates.

Endocytosis of EphA2 could potentially limit Src diffusion along the plasma membrane in a real cell–cell contact. However, the endocytosis of membrane:membrane complexes is generally much slower than soluble ligand:receptor complexes; therefore, we do not expect that endocytosis of EphA2 plays a major role in Src dynamics reported here. One remaining question concerns how long can a Src molecule maintain its active state when diffusing out of EphA2 receptors. Src inactivation is regulated by two kinetic reactions: dephosphorylation of active loop Y419 by protein tyrosine phosphate PTP-BAS (61), and phosphorylation of autoinhibitory loop Y530 by protein tyrosine kinase Csk (62). Whether EphA2 signaling will interfere with these two regulators is also not known. Further study on the timescale of Src inactivation will help to understand more precisely about the spatiotemporal regulation of EphA2 signaling and integrin functions.

Recent studies suggest that EphA2 signaling involves a balance between ligand-dependent and ligand-independent activity (13–16).

While ligand-independent signaling through serine phosphorylation is believed to promote tumor progression (13), our results here suggest that ligand-dependent signaling through tyrosine phosphorylation also promotes cell motility in a spatially controlled manner. Overall, we suggest that spatial distribution of ephrinA1 ligand is an integral aspect of the EphA2 signaling system.

Materials and Methods

Patterned substrate of fluid ephrinA1 and immobilized RGD, and cell culture and plasmids are described in *SI Appendix, Materials and Methods*.

Immunostaining and Western blotting follow standard protocols described in *SI Appendix, Materials and Methods*.

Cell imaging and image analysis are described in *SI Appendix, Materials and Methods*.

ACKNOWLEDGMENTS. We thank Dr. Bai Funing and Ms. Ong Huiting for their help with Matlab programming. We also thank Dr. Adrienne Greene (J.T.G. laboratory, University of California, Berkeley) for her contribution of purified ephrinA1 protein, as well as helpful discussions. We thank Dr. Kevin Hartman's help in the beginning of this project. We thank other members in J.T.G. laboratory, R.Z.-B. laboratory, and Michael Sheetz laboratory for stimulating discussions and sharing of reagents. This work was supported by National Institutes of Health National Cancer Institute Physical Sciences in Oncology Network Project 1-U01CA202241. Collaborative work at the Mechanobiology Institute, National University of Singapore, was supported by CRP001-084.

1. Fox BP, Kandpal RP (2004) Invasiveness of breast carcinoma cells and transcript profile: Eph receptors and ephrin ligands as molecular markers of potential diagnostic and prognostic application. *Biochem Biophys Res Commun* 318:882–892.
2. Sugiyama N, et al. (2013) EphA2 cleavage by MT1-MMP triggers single cancer cell invasion via homotypic cell repulsion. *J Cell Biol* 201:467–484.
3. Zelinski DP, Zantek ND, Stewart JC, Irizarry AR, Kinch MS (2001) EphA2 overexpression causes tumorigenesis of mammary epithelial cells. *Cancer Res* 61:2301–2306.
4. Ireton RC, Chen J (2005) EphA2 receptor tyrosine kinase as a promising target for cancer therapeutics. *Curr Cancer Drug Targets* 5:149–157.
5. Pan M (2005) Overexpression of EphA2 gene in invasive human breast cancer and its association with hormone receptor status. *J Clin Oncol* 23:9583.
6. Fang WB, Brantley-Sieders DM, Parker MA, Reith AD, Chen J (2005) A kinase-dependent role for EphA2 receptor in promoting tumor growth and metastasis. *Oncogene* 24:7859–7868.
7. Brantley-Sieders DM, et al. (2008) The receptor tyrosine kinase EphA2 promotes mammary adenocarcinoma tumorigenesis and metastatic progression in mice by amplifying ErbB2 signaling. *J Clin Invest* 118:64–78.
8. Macrae M, et al. (2005) A conditional feedback loop regulates Ras activity through EphA2. *Cancer Cell* 8:111–118.
9. Yang N-Y, et al. (2011) Crosstalk of the EphA2 receptor with a serine/threonine phosphatase suppresses the Akt-mTORC1 pathway in cancer cells. *Cell Signal* 23: 201–212.
10. Miao H, Burnett E, Kinch M, Simon E, Wang B (2000) Activation of EphA2 kinase suppresses integrin function and causes focal-adhesion-kinase dephosphorylation. *Nat Cell Biol* 2:62–69.
11. Deroanne C, Vouret-Craviari V, Wang B, Pouysségur J (2003) EphrinA1 inactivates integrin-mediated vascular smooth muscle cell spreading via the Rac/PAK pathway. *J Cell Sci* 116:1367–1376.
12. Fero D, et al. (2011) Ephrin-A1 regulates cell remodeling and migration. *Cell Mol Bioeng* 4:648–655.
13. Miao H, et al. (2009) EphA2 mediates ligand-dependent inhibition and ligand-independent promotion of cell migration and invasion via a reciprocal regulatory loop with Akt. *Cancer Cell* 16:9–20.
14. Barquilla A, et al. (2016) Protein kinase A can block EphA2 receptor-mediated cell repulsion by increasing EphA2 S897 phosphorylation. *Mol Biol Cell* 27:2757–2770.
15. Paraiso KHT, et al. (2015) Ligand-independent EPHA2 signaling drives the adoption of a targeted therapy-mediated metastatic melanoma phenotype. *Cancer Discov* 5:264–273.
16. Zhou Y, et al. (2015) Crucial roles of RSK in cell motility by catalysing serine phosphorylation of EphA2. *Nat Commun* 6:7679.
17. Salaita K, et al. (2010) Restriction of receptor movement alters cellular response: Physical force sensing by EphA2. *Science* 327:1380–1385.
18. Lohmüller T, Xu Q, Groves JT (2013) Nanoscale obstacle arrays frustrate transport of EphA2–Ephrin-A1 clusters in cancer cell lines. *Nano Lett* 13:3059–3064.
19. Greene AC, et al. (2014) Spatial organization of EphA2 at the cell-cell interface modulates trans-endocytosis of ephrinA1. *Biophys J* 106:2196–2205.
20. Groves JT, Ulman N, Boxer SG (1997) Micropatterning fluid lipid bilayers on solid supports. *Science* 275:651–653.
21. Groves JT, Boxer SG (2002) Micropattern formation in supported lipid membranes. *Acc Chem Res* 35:149–157.
22. Zamir E, Geiger B (2001) Molecular complexity and dynamics of cell-matrix adhesions. *J Cell Sci* 114:3583–3590.
23. Walsh R, Blumenberg M (2011) Specific and shared targets of ephrin A signaling in epidermal keratinocytes. *J Biol Chem* 286:9419–9428.
24. Afshari FT, Kwok JC, Fawcett JW (2010) Astrocyte-produced ephrins inhibit Schwann cell migration via VAV2 signaling. *J Neurosci* 30:4246–4255.
25. Yamazaki T, et al. (2009) EphA1 interacts with integrin-linked kinase and regulates cell morphology and motility. *J Cell Sci* 122:243–255.
26. Saeki N, Nishino S, Shimizu T, Ogawa K (2015) EphA2 promotes cell adhesion and spreading of monocyte and monocyte/macrophage cell lines on integrin ligand-coated surfaces. *Cell Adhes Migr* 9:469–482.
27. Wimmer-Kleikamp SH, et al. (2008) Elevated protein tyrosine phosphatase activity provokes Eph/ephrin-facilitated adhesion of pre-B leukemia cells. *Blood* 112:721–732.
28. Parri M, et al. (2007) EphrinA1 activates a Src/focal adhesion kinase-mediated motility response leading to rho-dependent actino/myosin contractility. *J Biol Chem* 282:19619–19628.
29. Carter N, Nakamoto T, Hirai H, Hunter T (2002) EphrinA1-induced cytoskeletal reorganization requires FAK and p130(cas). *Nat Cell Biol* 4:565–573.
30. Miao H, Wang B (2012) EphA receptor signaling–Complexity and emerging themes. *Semin Cell Dev Biol* 23:16–25.
31. Yu CH, Law JBK, Suryana M, Low HY, Sheetz MP (2011) Early integrin binding to Arg-Gly-Asp peptide activates actin polymerization and contractile movement that stimulates outward translocation. *Proc Natl Acad Sci USA* 108:20585–20590.
32. Mossman KD, Campi G, Groves JT, Dustin ML (2005) Altered TCR signaling from geometrically repatterned immunological synapses. *Science* 310:1191–1193.
33. Manz BN, Jackson BL, Petit RS, Dustin ML, Groves J (2011) T-cell triggering thresholds are modulated by the number of antigen within individual T-cell receptor clusters. *Proc Natl Acad Sci USA* 108:9089–9094.
34. Nye JA, Groves JT (2008) Kinetic control of histidine-tagged protein surface density on supported lipid bilayers. *Langmuir* 24:4145–4149.
35. Parri M, et al. (2005) EphrinA1 repulsive response is regulated by an EphA2 tyrosine phosphatase. *J Biol Chem* 280:34008–34018.
36. Walker-Daniels J, Riese DJ, 2nd, Kinch MS (2002) c-Cbl-dependent EphA2 protein degradation is induced by ligand binding. *Mol Cancer Res* 1:79–87.
37. Pratt RL, Kinch MS (2002) Activation of the EphA2 tyrosine kinase stimulates the MAP/ERK kinase signaling cascade. *Oncogene* 21:7690–7699.
38. Mohamed AM, Boudreau JR, Yu FPS, Liu J, Chin-Sang ID (2012) The *Caenorhabditis elegans* Eph receptor activates NCK and N-WASP, and inhibits Ena/VASP to regulate growth cone dynamics during axon guidance. *PLoS Genet* 8:e1002513.
39. Prager-Khoutorsky M, et al. (2011) Fibroblast polarization is a matrix-rigidity-dependent process controlled by focal adhesion mechanosensing. *Nat Cell Biol* 13: 1457–1465.
40. Gauthier NC, Masters TA, Sheetz MP (2012) Mechanical feedback between membrane tension and dynamics. *Trends Cell Biol* 22:527–535.
41. Wakefield DL, Holowka D, Baird B (2017) The FcεRI signaling cascade and integrin trafficking converge at patterned ligand surfaces. *Mol Biol Cell* 28:3383–3396.
42. Carroll-Portillo A, et al. (2015) Mast cells and dendritic cells form synapses that facilitate antigen transfer for T cell activation. *J Cell Biol* 210:851–864.
43. Pierini LM, Lawson MA, Eddy RJ, Hendey B, Maxfield FR (2000) Oriented endocytic recycling of α5β1 in motile neutrophils. *Blood* 95:2471–2480.
44. Bretscher MS (1992) Circulating integrins: Alpha 5 beta 1, alpha 6 beta 4 and Mac-1, but not alpha 3 beta 1, alpha 4 beta 1 or LFA-1. *EMBO J* 11:405–410.
45. Knöll B, Drescher U (2004) Src family kinases are involved in EphA receptor-mediated retinal axon guidance. *J Neurosci* 24:6248–6257.
46. Roskoski R, Jr (2015) Src protein-tyrosine kinase structure, mechanism, and small molecule inhibitors. *Pharmacol Res* 94:9–25.
47. Guarino M (2010) Src signaling in cancer invasion. *J Cell Physiol* 223:14–26.
48. Brunton VG, et al. (2005) Identification of Src-specific phosphorylation site on focal adhesion kinase: Dissection of the role of Src SH2 and catalytic functions and their consequences for tumor cell behavior. *Cancer Res* 65:1335–1342.
49. Mitra SK, Hanson DA, Schlaepfer DD (2005) Focal adhesion kinase: In command and control of cell motility. *Nat Rev Mol Cell Biol* 6:56–68.
50. Zaidel-Bar R, Milo R, Kam Z, Geiger B (2007) A paxillin tyrosine phosphorylation switch regulates the assembly and form of cell-matrix adhesions. *J Cell Sci* 120:137–148.
51. Bartley TD, et al. (1994) B61 is a ligand for the ECK receptor protein-tyrosine kinase. *Nature* 368:558–560.
52. Hirai H, Maru Y, Hagiwara K, Nishida J, Takaku F (1987) A novel putative tyrosine kinase receptor encoded by the eph gene. *Science* 238:1717–1720.
53. Natkanski E, et al. (2013) B cells use mechanical energy to discriminate antigen affinities. *Science* 340:1587–1590.
54. Gordon WR, et al. (2015) Mechanical allostery: Evidence for a force requirement in the proteolytic activation of notch. *Dev Cell* 33:729–736.
55. Davis S, et al. (1994) Ligands for EPH-related receptor tyrosine kinases that require membrane attachment or clustering for activity. *Science* 266:816–819.
56. Jørgensen C, et al. (2009) Cell-specific information processing in segregating populations of Eph receptor ephrin-expressing cells. *Science* 326:1502–1509.
57. Sahin M, et al. (2005) Eph-dependent tyrosine phosphorylation of ephexin1 modulates growth cone collapse. *Neuron* 46:191–204.
58. Shamah SM, et al. (2001) EphA receptors regulate growth cone dynamics through the novel guanine nucleotide exchange factor ephexin. *Cell* 105:233–244.
59. Deramaudt TB, et al. (2011) FAK phosphorylation at Tyr-925 regulates cross-talk between focal adhesion turnover and cell protrusion. *Mol Biol Cell* 22:964–975.
60. Lee HH, et al. (2010) Src-dependent phosphorylation of ROCK participates in regulation of focal adhesion dynamics. *J Cell Sci* 123:3368–3377.
61. Roskoski R, Jr (2005) Src kinase regulation by phosphorylation and dephosphorylation. *Biochem Biophys Res Commun* 331:1–14.
62. Okada M, Nakagawa H (1989) A protein tyrosine kinase involved in regulation of pp60c-src function. *J Biol Chem* 264:20886–20893.